NeuroImage 109 (2015) 249–259

Contents lists available at ScienceDirect

NeuroImage

journal homepage: www.elsevier.com/locate/ynimg

Upright face-preferential high-gamma responses in lower-order visual areas: Evidence from intracranial recordings in children

Naoyuki Matsuzaki [a], Rebecca F. Schwarzlose [c,e], Masaaki Nishida [a,d], Noa Ofen [a,c], Eishi Asano [a,b,*]

[a] Department of Pediatrics, Children's Hospital of Michigan, Wayne State University, Detroit Medical Center, Detroit, MI 48201, USA
[b] Department of Neurology, Children's Hospital of Michigan, Wayne State University, Detroit Medical Center, Detroit, MI 48201, USA
[c] Institute of Gerontology, Wayne State University, Detroit, MI, USA
[d] Department of Anesthesiology, Hanyu General Hospital, Hanyu City, Saitama 348-8505, Japan
[e] Trends in Cognitive Sciences, Cell Press, Cambridge, MA 02139, USA

ARTICLE INFO

Article history:
Accepted 5 January 2015
Available online 9 January 2015

Keywords:
High-frequency oscillations (HFOs)
Ripples
Intracranial recording
Category-specific responses
Pediatric epilepsy surgery
ECoG

ABSTRACT

Behavioral studies demonstrate that a face presented in the upright orientation attracts attention more rapidly than an inverted face. Saccades toward an upright face take place in 100–140 ms following presentation. The present study using electrocorticography determined whether upright face-preferential neural activation, as reflected by augmentation of high-gamma activity at 80–150 Hz, involved the lower-order visual cortex within the first 100 ms post-stimulus presentation. Sampled lower-order visual areas were verified by the induction of phosphenes upon electrical stimulation. These areas resided in the lateral-occipital, lingual, and cuneus gyri along the calcarine sulcus, roughly corresponding to V1 and V2. Measurement of high-gamma augmentation during central (circular) and peripheral (annular) checkerboard reversal pattern stimulation indicated that central-field stimuli were processed by the more polar surface whereas peripheral-field stimuli by the more anterior medial surface. Upright face stimuli, compared to inverted ones, elicited up to 23% larger augmentation of high-gamma activity in the lower-order visual regions at 40–90 ms. Upright face-preferential high-gamma augmentation was more highly correlated with high-gamma augmentation for central than peripheral stimuli. Our observations are consistent with the hypothesis that lower-order visual regions, especially those for the central field, are involved in visual cues for rapid detection of upright face stimuli.

Introduction

The human brain has a remarkable ability to efficiently recognize faces. Behavioral studies have shown that picture stimuli containing the faces of living things, compared to those with other non-face objects, more rapidly attract gazes from healthy participants, including infants (Quinn and Eimas, 1998) and adults (Kirchner and Thorpe, 2006; Fletcher-Watson et al., 2008). Among the most investigated features of human face recognition is its selectivity to upright orientation (Farah et al., 1998; Haxby et al., 1999; Yovel and Kanwisher, 2004). A face presented in the upright orientation, compared to one flipped upside down, is more easily recognized and automatically draws earlier and more sustained attention from healthy infants (Valenza et al., 1996; Quinn et al., 2009) and adults (Hochberg and Galper, 1967; Yin, 1969). Furthermore, preferential saccades toward an upright face take place within 100–140 ms following presentation (Kirchner and Thorpe, 2006; Crouzet et al., 2010), demonstrating that detection of an upright face occurs quite early in visual processing.

Neural correlates of face recognition have been extensively examined using functional MRI (fMRI) (Puce et al., 1995; Kanwisher et al., 1997; Summerfield et al., 2006; Mendola and Buckthought, 2013) and electrocorticography (ECoG) (Miller et al., 2009; Engell and McCarthy, 2010; Vidal et al., 2010). These studies have consistently localized regions of face-selectivity around the fusiform and inferior occipital gyri. Disruption of the region around the inferior occipital gyrus using repetitive transcranial magnetic stimulation (rTMS) at 60 and 100 ms after presentation of face stimuli impairs performance on a discrimination task with face parts, demonstrating the early involvement of face-selective areas in face processing (Pitcher et al., 2007). Combined with the observed preferential saccades to upright faces within 100 and 140 ms of stimulus presentation (Kirchner and Thorpe, 2006; Crouzet et al., 2010), these short timescales highlight the rapid nature of face detection and processing. Our knowledge of the time course of face processing is further informed by the findings from ECoG studies that activity for face stimuli, compared to non-face stimuli, elicit greater high-gamma augmentation in the ventral occipital–temporal junction at 200–300 ms after the onset of stimulus presentation (Engell and McCarthy, 2010; Vidal et al., 2010).

* Corresponding author at: Division of Pediatric Neurology, Children's Hospital of Michigan, Wayne State University. 3901 Beaubien St., Detroit, MI 48201, USA. Fax: +1 313 745 0955.
E-mail address: eishi@pet.wayne.edu (E. Asano).

http://dx.doi.org/10.1016/j.neuroimage.2015.01.015
1053-8119/

The roles of lower-order visual cortex in face recognition have been relatively under-reported. Taking into account that speeded saccadic responses toward an upright face take place as early as 100 ms, it is feasible to hypothesize that the lower-order visual cortex is involved in low-level visual cues for saccades toward upright face stimuli at <100 ms (Crouzet et al., 2010; Rossion and Caharel, 2011). In the present study of patients with focal epilepsy who underwent chronic ECoG recording, we investigated this idea using event-related augmentation of high-gamma activity at >80 Hz as a surrogate marker of *in-situ* cortical activation. The strengths of measurement of ECoG high-gamma augmentation include: (i) 20 to >100 times better signal-to-noise ratio compared to noninvasive neurophysiology modality (Ball et al., 2009), (ii) a temporal resolution of <20 ms (Fukuda et al., 2008), and (iii) direct signal sampling from deep structures such as medial and inferior surfaces of the occipital lobes (Uematsu et al., 2013).

In this study, we specifically determined if upright compared to inverted face stimuli would elicit larger high-gamma augmentation in lower-order visual sites at <100 ms following stimuli presentation. We hypothesized that upright face-preferential high-gamma augmentation would involve the lower-order visual regions, especially the portions of these regions dedicated to the central rather than the peripheral field, as humans tend to fixate face parts (such as eyes, nose, and mouth) rather than the facial contour or peripheral background during natural viewing (Birmingham et al., 2013; Vaidya et al., 2014).

Methods

Patients

The inclusion criteria of the present study included: (i) extraoperative ECoG recording as a part of clinical management of medically-uncontrolled seizures at Children's Hospital of Michigan in Detroit, (ii) ECoG sampling from the occipital and occipital–temporal regions, (iii) completion of a visual task described below, and (iv) age of 5 years and above. The exclusion criteria included: (i) brain malformations or seizure onset zone involving the occipital lobe, (ii) oculomotor dysfunction or visual field deficits detected by confrontation, and (iii) severe cognitive dysfunction reflected by verbal comprehension index of <70. The study was approved by the Institutional Review Board at Wayne State University, and written informed consent was obtained from the guardians of all participants.

Subdural electrode placement

Platinum grid and strip electrodes (10 mm intercontact distance, 4 mm diameter) were surgically implanted for extraoperative ECoG recording (Fig. 1; Asano et al., 2009a). All electrode plates were stitched to adjacent plates and/or the edge of dura mater, to avoid movement of subdural electrodes after placement. Intraoperative pictures were taken with a digital camera before dural closure. Planar x-ray images (lateral and anteroposterior) were subsequently acquired with the subdural electrodes in place for electrode localization on the brain surface (Miller et al., 2007; Muzik et al., 2007; Dalal et al., 2008); three metallic fiducial markers were placed at anatomically well-defined locations on the patient's head for co-registration of the x-ray image with the T1-weighted spoiled gradient echo MR image. A three-dimensional surface image was finally created with the location of electrodes directly defined on the brain surface (Muzik et al., 2007; Alkonyi et al., 2009). We confirmed the spatial accuracy of electrode display on the three-dimensional brain surface image using intraoperative pictures (Wellmer et al., 2002; Dalal et al., 2008; Pieters et al., 2013). By the age of 5 years, brain size becomes comparable to that of an adult (Dekaban and Sadowsky, 1978), while the youngest patient in the present study was 9 year old. Automatic parcellation of cortical gyri was performed using FreeSurfer software (Desikan et al., 2006), and subdural electrodes were assigned anatomical labels (Pieters et al., 2013; Fig. 1). The regions of interest in the present study included: (i) lingual gyrus, (ii) cuneus gyrus, (iii) lateral occipital region, and (iv) fusiform gyrus posterior to the midbrain (Desikan et al., 2006).

Localization of lower-order visual function by electrical stimulation

We localized lower-order visual areas with electrical stimulation mapping performed as a part of presurgical evaluation of medically uncontrolled focal seizures (Asano et al., 2009b; Zijlmans et al., 2009; Kumar et al., 2012). In short, we defined the lower-order visual areas as the sites at which stimulation constantly resulted in phosphene, or percepts of simple shape, color, or flush light (Murphey et al., 2009; Kim et al., 2013). Areas were not treated as lower-order visual areas if their stimulation elicited other types of visual symptoms, such as distortion (Parvizi et al., 2012). We expected that lower-order visual function would involve the lingual, cuneus, and lateral occipital regions close to the calcarine sulcus.

A train of repetitive electrical stimuli was delivered to a pair of subdural electrodes using the Grass stimulator (Astro-Med, Inc, West Warwick, RI), and clinical symptoms elicited by stimulation were observed by at least two investigators including a neuropsychologist. The stimulus frequency was 50 Hz, the pulse duration was 300 μs, and the train duration ranged up to 2 s. To determine the presence of after-discharges, video-ECoG was recorded continuously during the entire mapping session. When a clinical symptom was elicited, the train of stimuli was immediately terminated. Stimulus intensity was initially set to 3 mA and was increased to 6 and 9 mA in a stepwise manner until a clinical symptom or after-discharge was observed. Once the after-discharge threshold was determined, stimulus intensity above that threshold was no longer utilized. Sites at which stimulation consistently (at least twice) elicited a clinical symptom were classified as eloquent areas specific to a given symptom. Sites were declared 'not proven to be eloquent' if after-discharges were elicited without a symptom, or a symptom failed to be elicited by maximal stimuli. To minimize worry or fear on the part of the patient, each individual was informed prior to the stimulation study that she/he might have a transient sensorimotor, auditory, visual, olfactory, gustatory, or language symptom. Each patient was aware of the timing of each stimulation trial but unaware of the location of stimulated sites.

Extraoperative ECoG recording

Extraoperative video-ECoG recordings were obtained using a 192-channel Nihon Kohden Neurofax 1100A Digital System (Nihon Kohden America Inc, Foothill Ranch, CA, USA). The sampling frequency was set at 1000 Hz with the amplifier band pass at 0.08–300 Hz (Kojima et al., 2013a). The averaged voltage of ECoG signals derived from the fifth and sixth intracranial electrodes of the ECoG amplifier was used as the original reference. ECoG signals were then re-montaged to a common average reference (Korzeniewska et al., 2011; Wu et al., 2011). Channels contaminated with large interictal epileptiform discharges or artifacts were excluded from the common average reference. No notch filter was used. All antiepileptic medications were discontinued on the day of subdural electrode placement. Electrodes overlying seizure onset zones or structural lesions were excluded from further analysis (Jacobs et al., 2009). Surface EMG electrodes were placed on the left and right deltoid muscles, and electrooculography (EOG) electrodes were placed 2.5 cm below and 2.5 cm lateral to the left and right outer canthi.

Task

During video-ECoG recording, a series of visual stimuli were presented to each patient using a 22-inch Dell P2213 LCD monitor (a refresh rate of 60 Hz; a pixel resolution of 1600 × 1050; Dell Inc, Round Rock, TX, USA) placed 60 cm away from the patient. The task lasted approximately four minutes. Each patient completed the task while awake, unsedated, and comfortably seated on the bed in a

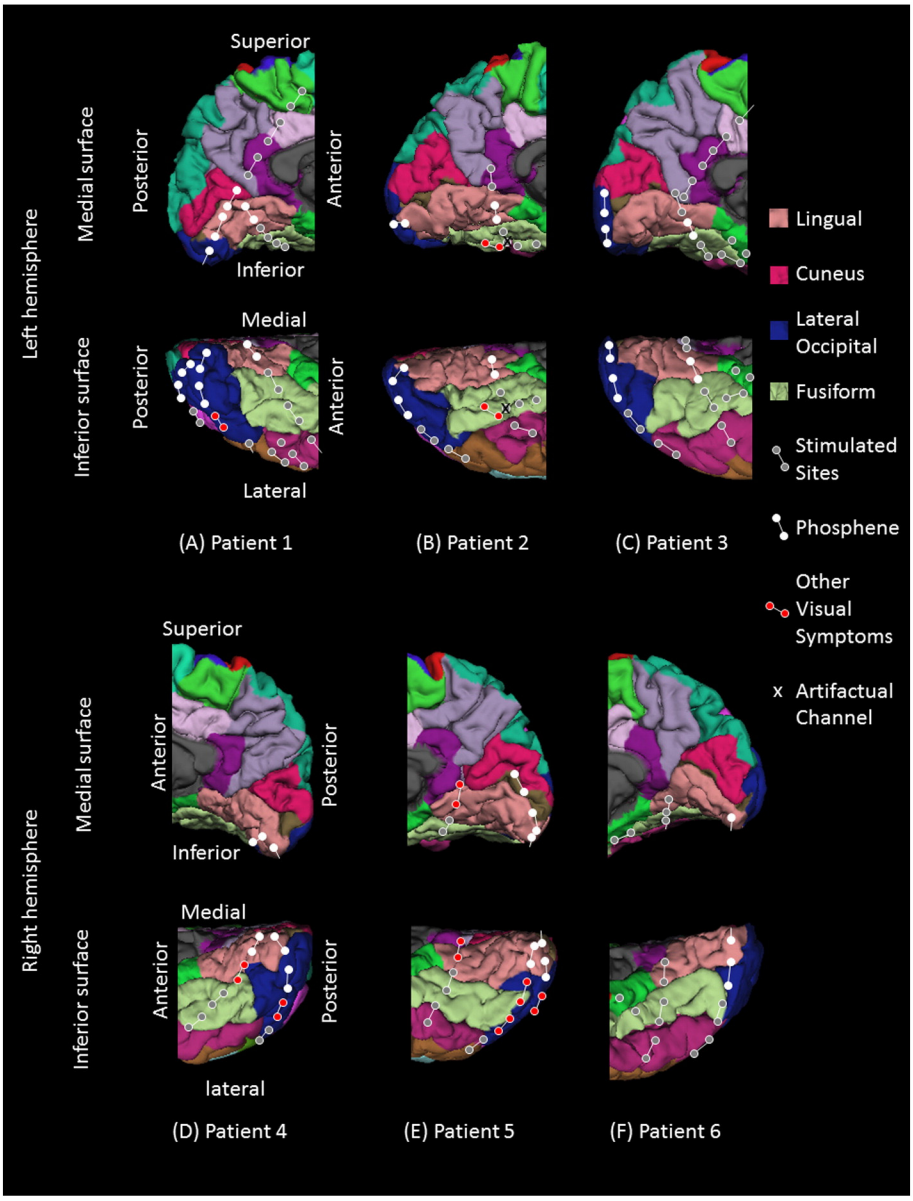

Fig. 1. Location of subdural electrodes over the occipital–temporal regions. (A) Patient 1. (B) Patient 2. (C) Patient 3. (D) Patient 4. (E) Patient 5. (F) Patient 6. Cortical gyri were parcellated and color coded using FreeSurfer software (Desikan et al., 2006). White circles: sites of which stimulation resulted in phosphene. Red circles: sites of which stimulation resulted in other visual percepts ("Objects looking funny" in Patient 1; "Funny looking" in Patient 2; "Background felt moving" during stimulation of lateral occipital sites in Patient 4; "I saw something but cannot tell what it is" during stimulation of a lingual–fusiform pair in Patient 4; "Something blurry and transparent but not anything" during stimulation of three pairs in the lateral-occipital regions and "something changes" during stimulation of lingual sites in Patient 5). Gray circles: sites of which stimulation resulted in no visual symptom. Circle with X: Electrode affected by artifacts (excluded from analysis).

dimly-lit room. Stimuli included a star-shaped drawing, upright faces, inverted faces, upright houses, a circular checkerboard reversal pattern, and an annular checkerboard reversal pattern (Fig. 2). Stimuli were binocularly presented in grayscale on a black background at the center of the monitor. They appeared in a pseudorandom order for a duration of 533 ms each, with an inter-stimulus interval ranging from 2.0 to 2.5 s. The order of presentation of stimuli was counterbalanced across image categories. Each patient was instructed to fixate on the center of the screen (indicated by the fixation cross of 1° height and width during the inter-stimulus interval), and to overtly say 'star' only when the target star-shaped drawing (size: 9 × 9°; color: white) was presented. No other action was required. Stimuli also included 40 faces and 40 houses (Ekman and Friesen, 1976; Woods et al., 2003). Each of the face and house stimuli was cropped into an oval-like shape (about 11° width and 16° height). Face stimuli were presented 40 times in the upright orientation and 40 times in the inverted orientation, whereas house stimuli were presented 40 times exclusively in the upright orientation. A black-and-white circular checkerboard reversal pattern (radius: 9.6°) and an annular checkerboard reversal pattern (inner radius: 9.6°; outer radius: 23°), each presented with a pulse duration of 133 ms and a train duration of 533 ms, were each presented four times. In other words, a total of 16 pulses of circular and annular checkerboard stimuli were presented to each patient to localize the lower-order visual cortex for the central and peripheral fields, respectively.

Measurement of event-related gamma activity

The general principle of our time-frequency analysis was previously reported (Brown et al., 2008; Nagasawa et al., 2011; Matsuzaki et al., 2012). In short, we determined the spatial-temporal dynamics of high-gamma amplitudes at 80–150 Hz following the onset of image presentation, and we believe this is a reasonable summary measure of

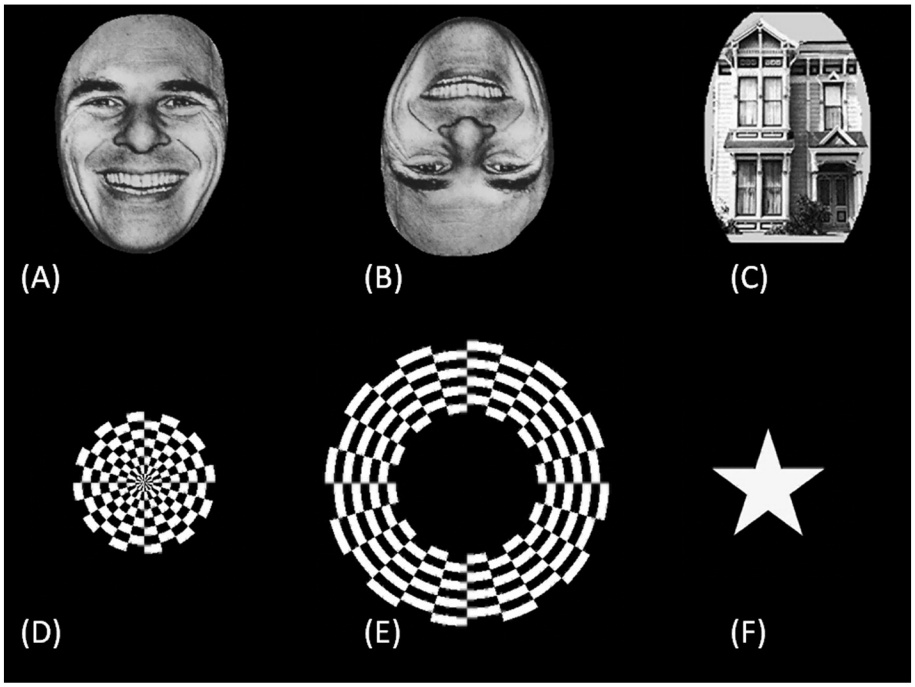

Fig. 2. Examples of visual stimuli. (A) Upright face. (B) Inverted face. (C) House. (D) Circular checkerboard pattern. (E) Annular checkerboard pattern. (F) Star shape.

in-situ cortical activity. A study of macaque monkeys using single-unit recordings suggested that task-related augmentation of high-gamma activity was tightly correlated to an increased firing rate (Ray et al., 2008). Our previous ECoG study of the effect of photic stimulation on the occipital cortex revealed that the earliest and largest amplitude augmentation involved the 80–150 Hz frequency band (Matsuzaki et al., 2012). The peak frequency of high-gamma modulations during various forms of sensorimotor and cognitive tasks also involved this frequency band (Nagasawa et al., 2011; Kojima et al., 2013b).

Each ECoG trial was transformed into the time–frequency domain using a complex demodulation technique (Papp and Ktonas, 1977) incorporated in BESA® EEG V.5.1.8 software (BESA GmbH, Gräfelfing, German; Hoechstetter et al., 2004). The time-frequency transform was obtained by multiplication of the time-domain signal with a complex exponential, followed by a low-pass filter. The low-pass filter used here was a finite impulse response filter of Gaussian shape, making the complex demodulation effectively equivalent to a Gabor transform. The filter had a full width at half maximum of 2×15.8 ms in the temporal domain and 2×7.1 Hz in the frequency domain. The corresponding time-frequency resolution was ± 15.8 ms and ± 7.1 Hz (defined as the 50% power drop of the finite impulse response filter). A given ECoG signal was assigned an amplitude (a measure proportional to the square root of power) as a function of time and frequency at each trial. Time-frequency transformation was performed for frequencies between 80 and 150 Hz and latencies between -800 and $+1000$ ms relative to the image presentation, in steps of 5 Hz and 10 ms. At each time-frequency bin, we analyzed the percent change in amplitude (averaged across trials) relative to the mean amplitude in a reference period at -800 to -600 ms relative to the onset of image presentation. Such a change in amplitude has been termed "temporal spectral evolution" (TSE) (Salmelin and Hari, 1994).

Statistical assessment of high-gamma activity preferentially elicited by upright face stimuli

Using the statistical software incorporated in IBM SPSS Statistics 22 (IBM Corp., Chicago, IL, USA), we subsequently determined whether the percent change of high-gamma activity at 90 ms differed between upright and inverted face stimuli as well as between lower-order visual regions and other sites. We hypothesized that upright face-preferential high-gamma augmentation occurred at this time because a behavioral study suggested preferential saccades toward an upright face occurred as early as 100 ms (Crouzet et al., 2010). This analysis was done using a linear mixed-model analysis, with 'stimulus category' (e.g., upright vs inverted face), 'phosphene' (presence or absence), and 'interaction between stimulus category and phosphene' as fixed effects, and with 'individual electrodes' as a random effect. Subsequently, estimates of fixed effects were plotted from 10 until 300 ms in order to determine when upright face-preferential high-gamma augmentation in the lower-order visual cortex was maximized. The level of significance was set at $p = 0.05$.

Relationship between high-gamma activities elicited by upright face and checkerboard stimuli

We determined whether high-gamma augmentation for upright faces coincided with central- or peripheral-field lower-order visual processing. The analysis was done using a linear mixed-model analysis as described above. Fixed factors here included circular and annular stimuli-related high-gamma augmentation (Fig. 3). Based upon previous observations (Yoshor et al., 2007; Asano et al., 2009b; Uematsu et al., 2013), we expected that central-field checkerboard stimuli would elicit the largest gamma augmentation in sites proximal to the occipital pole, whereas peripheral-field stimuli would elicit the largest augmentation in the medial occipital sites along the calcarine fissure. Thereby, we expected that upright face-preferential high-gamma augmentation would be more highly correlated with high-gamma augmentation induced by central than peripheral stimuli.

Results

Patient profiles

We studied six children with focal epilepsy (age range: 9–17 years; average age: 13.5 years; 3 females, Table 1) who satisfied the inclusion and exclusion criteria described above. All six children were right-handed and had normal or corrected-to-normal visual acuity. Across

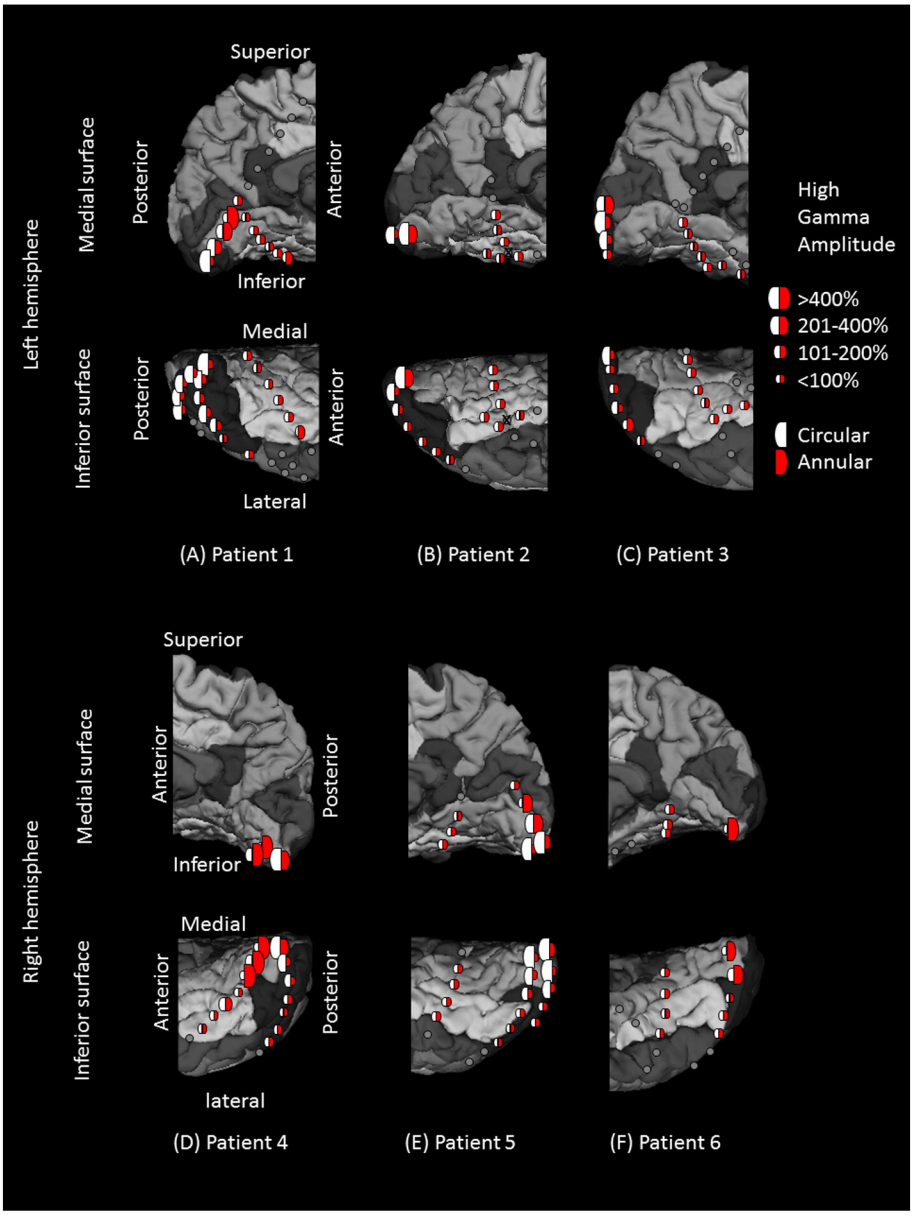

Fig. 3. High-gamma augmentation elicited by checkerboard pattern stimuli. (A) Patient 1. (B) Patient 2. (C) Patient 3. (D) Patient 4. (E) Patient 5. (F) Patient 6. White and red semicircles reflect the averaged percent change in high-gamma activity during circular (central) and annular (peripheral) checkerboard pattern stimulations, respectively. The degree of high-gamma augmentation elicited by central-field stimuli was larger in the region proximal to the occipital pole, while that by peripheral-field stimuli was larger in the more anterior medial surface of the occipital lobe. Gray circles: electrode sites outside the regions of interest. Gray circle with X: Electrode affected by artifacts (excluded from analysis).

patients, a total of 28, 3, 36, and 26 electrodes, free of artifacts, were located in the lingual gyrus, cuneus gyrus, lateral occipital region, and fusiform gyrus posterior to the midbrain, respectively (Fig. 1). All of these 93 electrodes were included for further analysis.

Table 1
Patient profile.

Patient	Age at surgery (years)	Antiepileptic medications	Sampled hemisphere	Seizure onset zone
1	14	LEV, OXC, LCM	Left	Not captured[a]
2	12	OXC, LEV, VPA	Left	Temporal
3	9	LEV, OXC	Left	Parietal
4	14	OXC, PHT	Right	Temporal
5	17	LCM, LEV	Right	Temporal
6	15	LMG, ZNS, LEV	Right	Temporal

LCM: Lacosamide. LEV: Levetiracetam. LMG: Lamotrigine. OXC: Oxcarbazepine. PHT: phenytoin. VPA: Valproic acid. ZNS: Zonisamide.
[a] Seizures were not captured, and a structural lesion in the left parietal lobe was removed.

Electrical stimulation data

Across patients, stimulation of 46 sites elicited phosphenes. These were classified as lower-order visual sites (21 in the lingual, 3 in the cuneus, 21 in the lateral-occipital, and 1 in the fusiform gyrus). The only fusiform site classified as a lower-order visual area was located very near to the lingual gyrus (Fig. 1). Visual assessment suggested that the lower-order visual sites defined by electrical stimulation in the present study lay within Brodmann Areas 17 and 18 (Amunts et al., 2000).

Stimulation of 15 sites elicited perception of some forms of visual distortion (2 in the lingual, 0 in the cuneus, 8 in the lateral occipital, and 5 in the fusiform gyrus) (Fig. 1). The percepts included: "Objects looking funny", "Background felt moving", "I saw something but cannot tell what it is", and "Something blurry and transparent but not anything".

The remaining 32 sites were not proven to be eloquent by electrical stimulation (4 in the lingual, 0 in the cuneus, 7 in the lateral occipital,

and 21 in the fusiform gyrus). The 2 by 4 Fisher Exact Probability Test suggested that the chance of stimulation-induced visual symptoms was greater in the lingual, cuneus, and lateral occipital regions, compared to in the fusiform gyrus ($p < 0.001$).

High-gamma augmentation elicited by checkerboard reversal pattern stimuli

Both circular (central-field) and annular (peripheral-field) checkerboard stimuli elicited high-gamma augmentation in the occipital lobe with the maximum peak amplitude in the lower-order visual sites defined by electrical stimulation (Fig. 3). A clear gradient of high-gamma amplitudes across sites in the anterior–posterior axis was noted; central-field stimuli were associated with largest high-gamma augmentation in the polar region, while peripheral-field stimuli with largest high-gamma augmentation in the anterior medial region (Fig. 3).

High-gamma augmentation preferentially elicited by upright, compared to inverted face stimuli

Examples of high-gamma augmentation elicited by upright and inverted faces are presented in Fig. 4. The temporal dynamics of such high-gamma activities in the lower-order visual sites as well as fusiform sites are presented in Fig. 5. A linear mixed-model analysis employed to upright and inverted face-related high-gamma augmentation at 90 ms revealed a significant effect of phosphene ($F = 37.4$; $p < 0.001$) and a significant interaction between phosphene and stimulus category ($F = 5.1$; $p = 0.027$); no significant effect of stimulus category was found ($F = 1.0$; $p = 0.76$). The fixed effect of phosphene on high-gamma augmentation was 0.98 (95% confidence interval [95%CI]: 0.61 to 1.35), whereas that of interaction between phosphene and upright face was 0.23 (95%CI: 0.027 to 0.44). In other words, lower-order visual sites, compared to the remaining sites, showed 98% larger high-gamma augmentation at 90 ms, and upright face stimuli, compared to inverted ones, showed 23% larger high-gamma augmentation only within the lower-order visual sites at the same moment. The plots of estimated fixed effects suggest that the effect of lower-order visual sites on high-gamma augmentation became larger than zero between 40 and 150 ms with a peak at 90 ms. Likewise, the effect of interaction between visual processing sites (lower-order versus others) and face orientation became larger than zero between 40 and 90 ms with the peak occurring at 80–90 ms (Fig. 6); namely, upright-face-preferential high-gamma augmentation in lower-order visual regions occurred within 100 ms of stimulus presentation and lasted for 50 ms. Fig. 7 shows relative high-gamma augmentation elicited by upright vs inverted faces at 40–90 ms at each electrode site, and we found that upright face-preferential high-gamma augmentation intensely involved the lower-order visual sites especially in the occipital pole.

Upright face-preferential high-gamma augmentation exerted by lower-order visual sites dedicated to the central rather than the peripheral field

The plots of estimated fixed effects on linear mixed-model analysis employed to upright and inverted face-related high-gamma

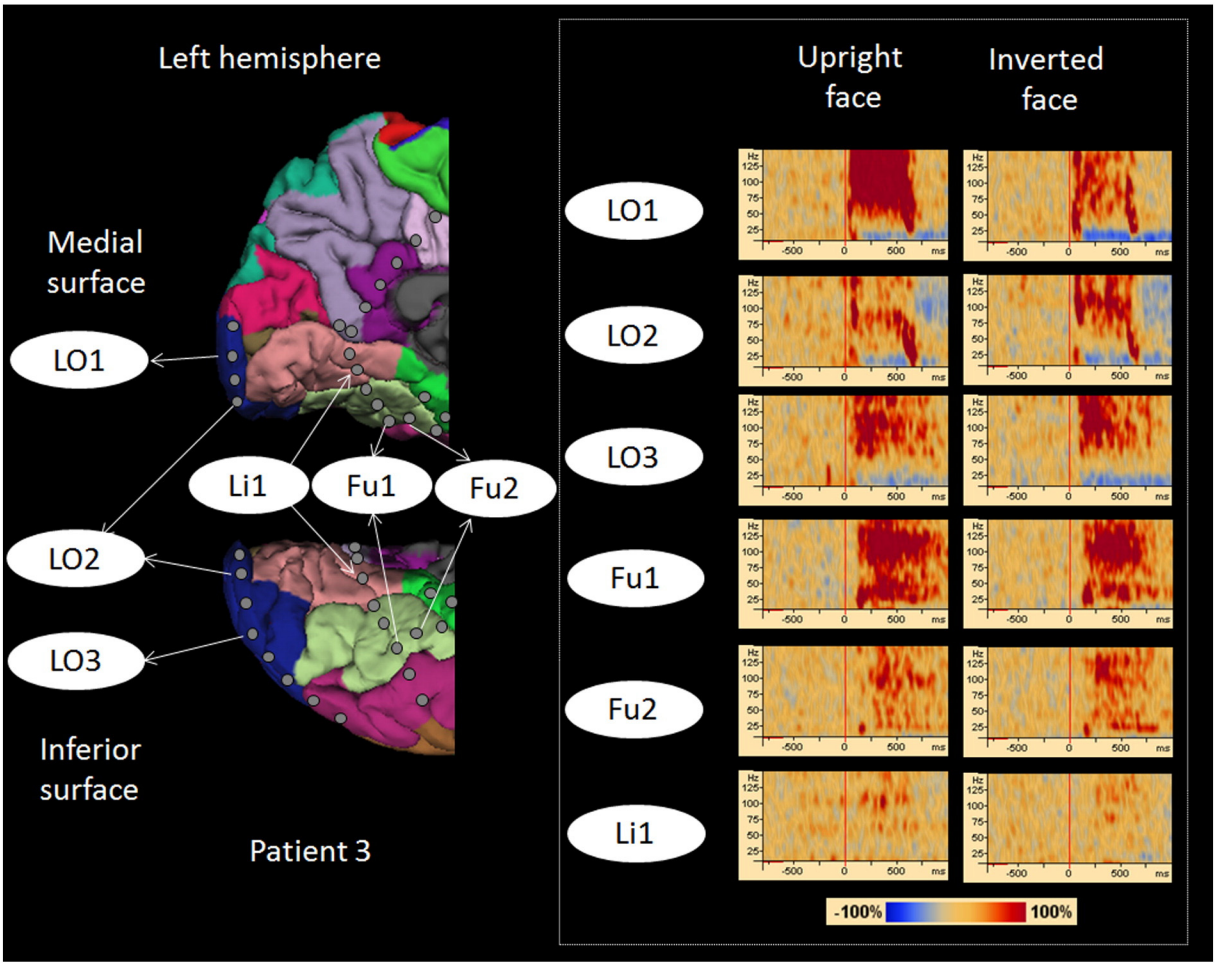

Fig. 4. High-gamma augmentation elicited by upright- and inverted-face stimuli. Time-frequency plots are presented in the right side. Both types of face stimuli elicited early high-gamma augmentation in lateral-occipital sites (Channels LO1, LO2, and LO3) and delayed augmentation in fusiform sites (Channels Fu1 and Fu2). High-gamma augmentation at a lingual site (Li1) was, if any, minimal. Upright face stimuli, compared to inverted ones, elicited larger high-gamma augmentation at Channel LO1.

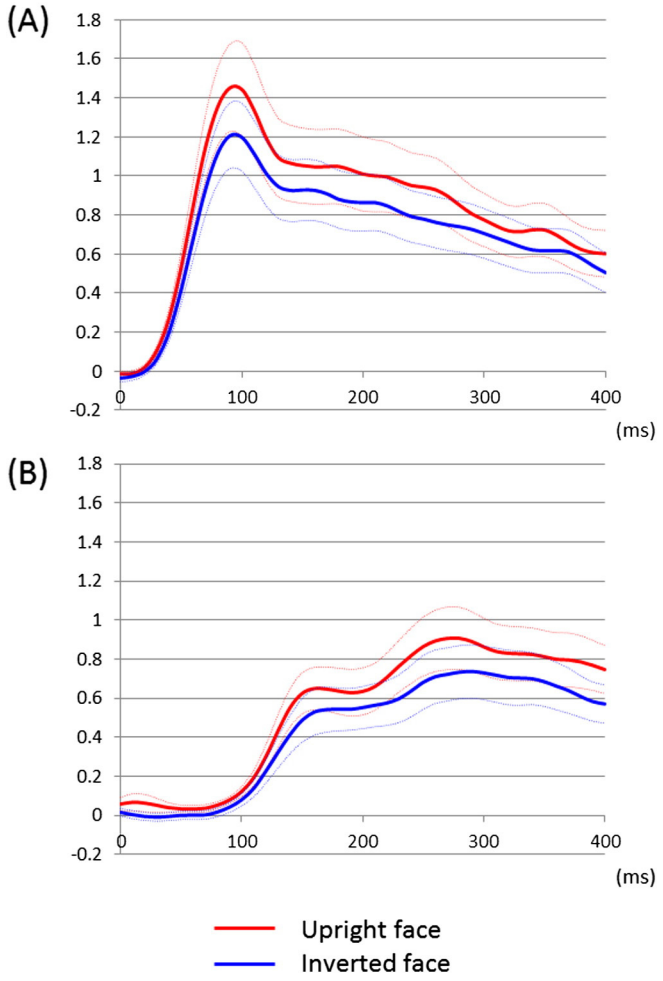

Fig. 5. Temporal dynamics of high-gamma augmentation elicited by upright- and inverted-face stimuli. (A) The mean high-gamma amplitudes across 46 lower-order visual sites are plotted over the time (red line: upright face; blue line: inverted face; dotted lines: mean ± standard error). Upright face stimuli, compared to inverted ones, elicited at least 20% larger high-gamma augmentation in lower-order visual sites at 70 to 110 ms. (B) The mean high-gamma amplitudes across 25 fusiform sites not associated with stimulation-induced phosphene are plotted over the time. High-gamma augmentation in these sites was minimal at <100 ms. Upright face stimuli, compared to inverted ones, elicited at least 15% larger high-gamma augmentation in such fusiform sites at 230 to 290 ms.

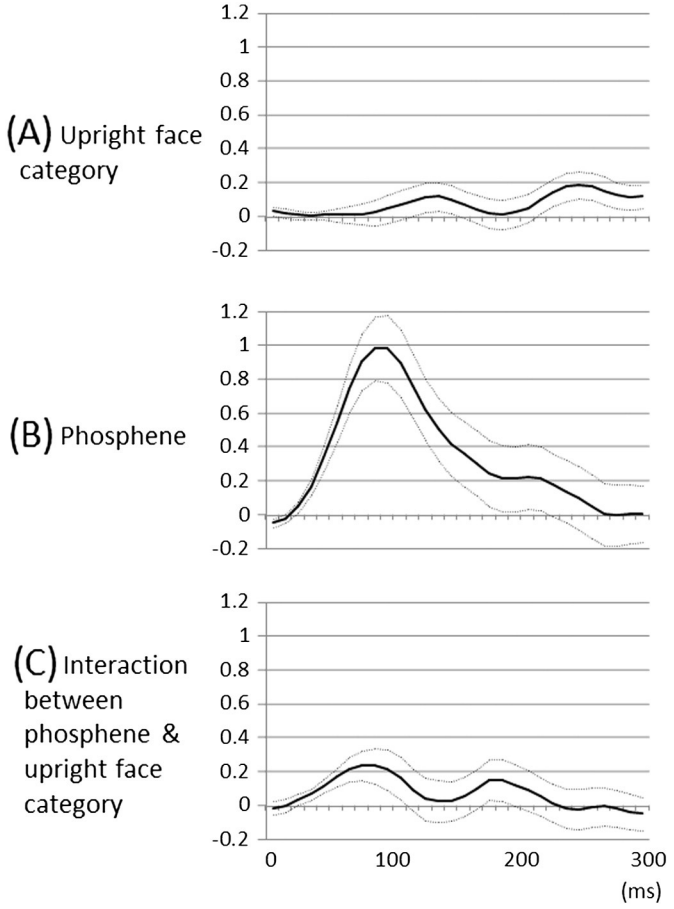

Fig. 6. Fixed effects of 'stimulus category' and 'underlying lower-order visual function' on high-gamma augmentation over the time course. (A) The linear mixed-model analysis suggested that the effect of upright face category on high-gamma augmentation became larger than zero at 240–260 ms, compared to that of inverted face. During this time period, upright face category was associated with larger high-gamma augmentation up to 18% compared to inverted face category, regardless of the underlying lower-order visual function. Solid line: estimated mean. Dotted lines: mean ± standard error. (B) Likewise, the effect of lower-order visual sites defined by stimulation-induced phosphene was larger than zero at 40–150 ms, compared to that of the remaining sites. During this period, lower-order visual sites were associated with larger high-gamma augmentation up to 98% compared to the remaining sites. (C) The effect of interaction between lower-order visual sites and upright face category became larger than zero at 40–90 ms. During this period, upright face stimuli elicited up to 23% larger high-gamma augmentation compared to inverted ones only within the lower-order visual sites.

augmentation are presented in Fig. 8. In short, 'upright face stimuli-preferential high-gamma augmentation' was correlated to 'high-gamma augmentation elicited by central-field checkerboard stimuli' better than to 'such augmentation elicited by peripheral-field stimuli'. The effect of interaction between central-field and upright face-preferential high-gamma augmentations was larger than zero between 50 and 300 ms (Fig. 8C), whereas the effect of interaction between peripheral-field and upright face-preferential high-gamma augmentations was larger than zero only between 70 and 90 ms (Fig. 8E). At 90 ms, each 100% increase in central-field-related high-gamma augmentation was associated with an 18% upright face-preferential high-gamma augmentation in a given site, whereas each 100% increase in peripheral-field-related high-gamma augmentation was associated with only a 6% upright face-preferential high-gamma augmentation.

Relationship between upper/lower visual fields and upright face-preferential high-gamma augmentation

As a post-hoc analysis, we determined if upright face-preferential high-gamma augmentation (relative to inverted face stimuli) in lower-order visual sites could have been simply attributed to the location of electrode sites relative to the calcarine fissure. In general, the occipital cortex below the calcarine fissure processes visual information in the upper field, while that above the calcarine fissure does so for the lower field (Horton and Hoyt, 1991; Schneider et al., 1993). We found that 8 and 38 out of the 46 lower-order visual sites were located above and below the calcarine fissures, respectively, in the present study.

We applied a linear mixed-model analysis to determine whether the percent change of high-gamma activity at 90 ms were associated with following fixed factors: 'stimulus category' (i.e.: upright vs inverted face), 'upper/lower visual fields' (i.e.: above vs below the calcarine fissure), and 'interaction between stimulus category and visual fields'. A significant effect of stimulus category ($F = 5.9$; $p = 0.02$) was found, but neither significant effect of visual fields ($F = 2.8$; $p = 0.1$) nor interaction between stimulus category and visual fields was found ($F = 0.2$; $p = 0.6$). We likewise explored if the percent change of high-gamma activity at 40–80 ms differed between the lower-order visual sites above and below the calcarine fissures. This linear mixed-

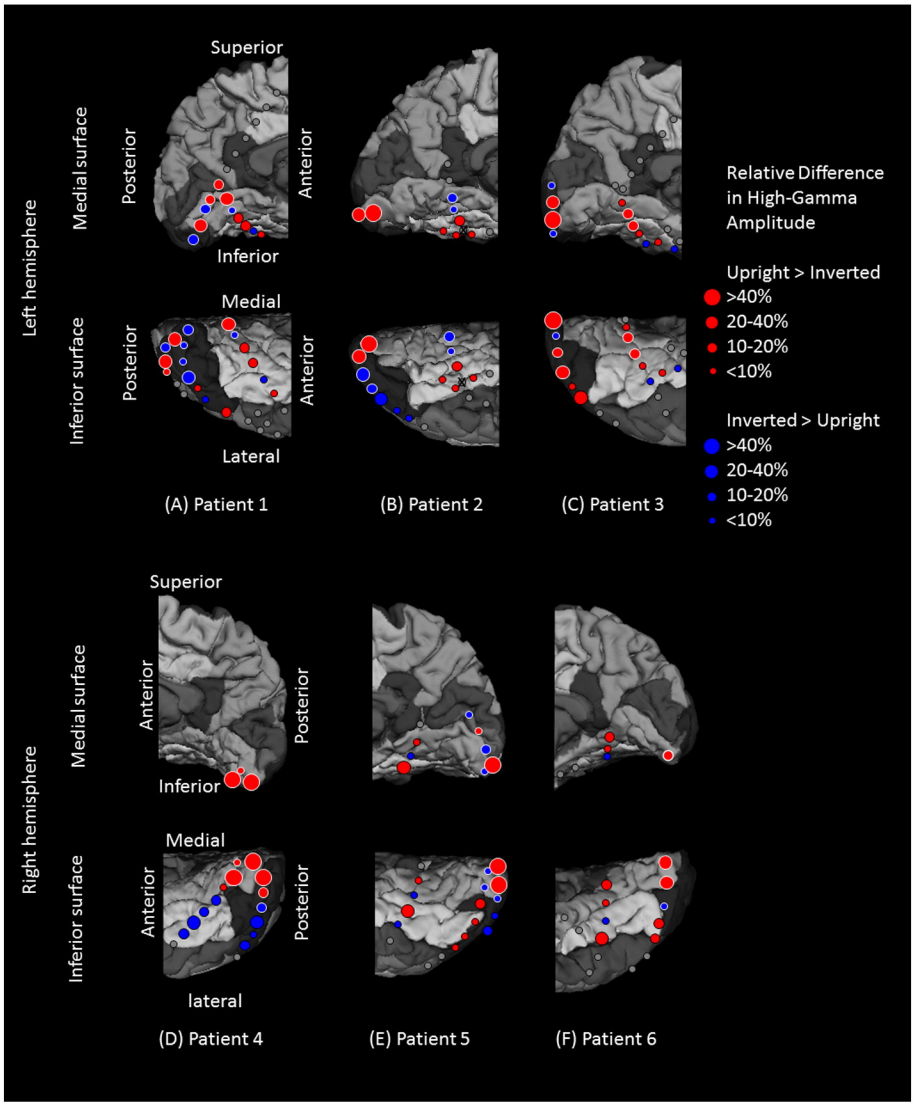

Fig. 7. Upright- and inverted-face-related high-gamma augmentation, at 40–90 ms, at individual electrode sites. Red filled circles: sites showing upright-face-related high-gamma augmentation larger than inverted-face-related one. Blue filled circles: sites showing inverted-face-related high-gamma augmentation larger than upright-face-related one. White rings: lower-order visual sites defined by electrical stimulation.

model analysis failed to find a significant effect of visual fields or interaction between stimulus category and visual fields ($p > 0.1$).

High-gamma augmentation elicited by upright face stimuli compared to house stimuli

The results are summarized in Supplementary Figure S1 and S2 (online material). In short, a linear mixed-model analysis suggested a significant positive effect of phosphene on high-gamma augmentation as well as a significant interaction between visual processing level of sites (lower-order versus other) and stimulus category; house stimuli, compared to upright faces, showed greater high-gamma augmentation within the lower-order visual sites. As best illustrated in Supplementary Figures S2C and S2E (online material), preferential high-gamma augmentation in response to house stimuli, compared with upright face stimuli, was correlated to that elicited by peripheral-field checkerboard stimuli better than that by central field.

Discussion

In this study, we identified a neural correlate of the face inversion effect within lower-order visual regions at a temporal range between 40 and 90 ms post-stimulus presentation. Our ECoG observation supports the hypotheses that the lower-order visual cortex is involved in preferential processing of upright face stimuli at <100 ms, and provides a plausible explanation for the behavioral observation that saccadic responses toward an upright face take place as early as 100 ms (Crouzet et al., 2010). We also demonstrated that upright face-preferential cortical activation was better correlated with lower-order visual function dedicated to the central field rather than that to the periphery. This finding is consistent with an fMRI observation that the BOLD response during face recognition is concentrated in the occipital–temporal visual pathway for the central visual field (Levy et al, 2001).

The ECoG effect of face inversion, taking place at a latency of 40–90 ms, is difficult to explain by the effect of feedback from higher-order visual areas. Our observation of such rapid category-specific neural activation in the lower-order visual regions can be incorporated into the conceptual framework for understanding feed-forward hierarchical processing in the visual system. We believe that such rapid upright face-preferential high-gamma augmentation may reflect the initial visual cues facilitating face detection rather than face recognition per se. Although the origins of this effect are not yet known, it may reflect a sensitivity at the earliest stages of cortical visual processing to

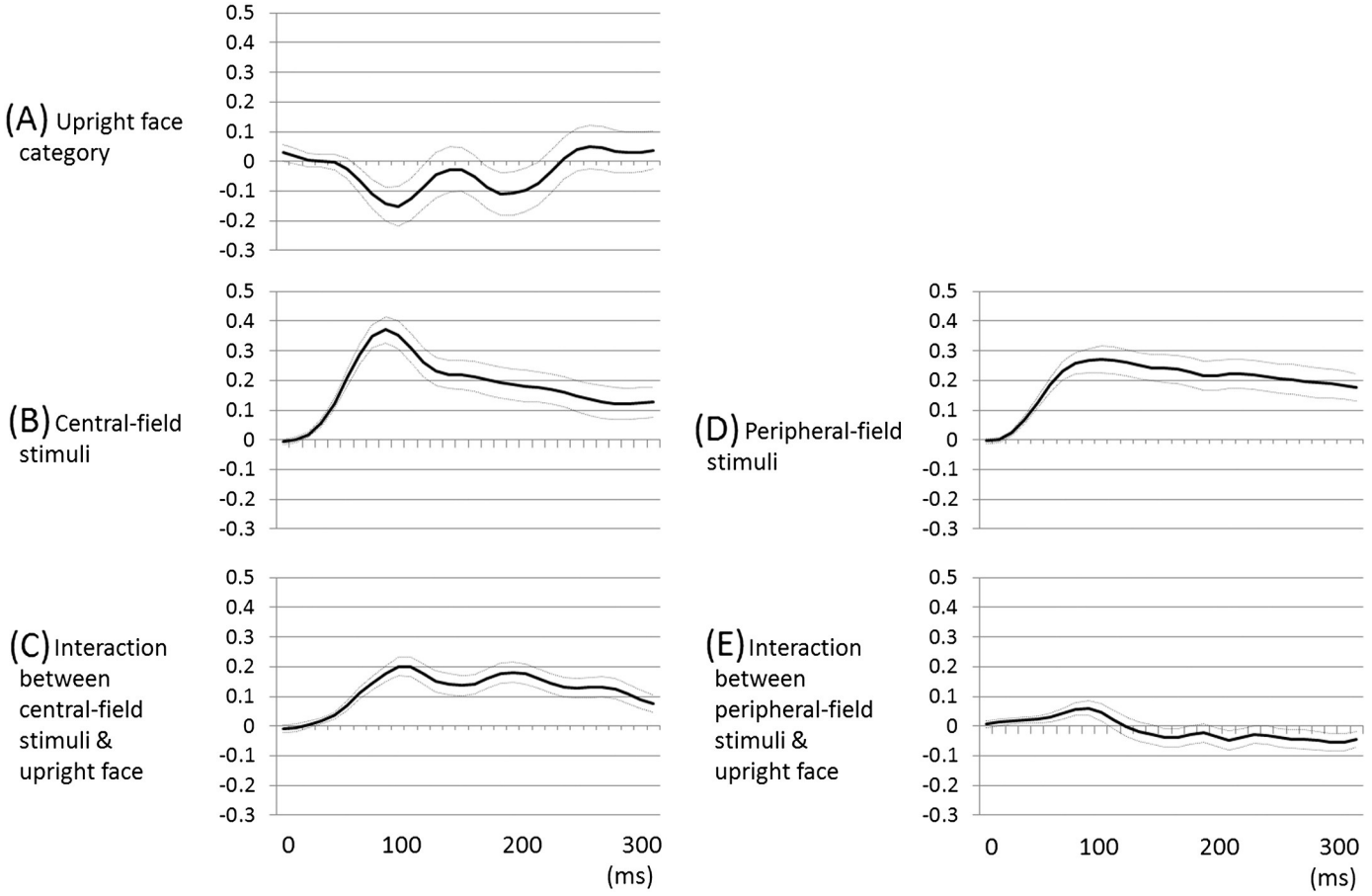

Fig. 8. Fixed effects of 'stimulus category' and 'cortical retinotopy' on high-gamma augmentation over the time course. (A) The effect of upright face category on high-gamma augmentation, compared to that of inverted face. (B) The effect of high-gamma augmentation elicited by central-field checkerboard stimulation. (C) The effect of interaction 'upright face category' and 'high-gamma augmentation elicited by central-field checkerboard stimulation'. At 90 ms, each 100% increase in central-field-related high-gamma augmentation was associated with an 18% upright face-preferential high-gamma augmentation in a given site. (D) The effect of high-gamma augmentation elicited by peripheral-field checkerboard stimulation. (E) The effect of interaction 'upright face category' and 'high-gamma augmentation elicited by peripheral-field checkerboard stimulation'. At 90 ms, each 100% increase in peripheral-field-related high-gamma augmentation was associated with a 6% upright face-preferential high-gamma augmentation in a given site.

the characteristic arrangement of low-level features signaling the presence of one of the most prevalent and salient stimuli that people encounter: 'the upright human face'. Indeed, it has been previously proposed that low-level amplitude spectrum patterns commonly seen in upright face stimuli would lead to rapid saccades toward upright face stimuli (Crouzet and Thorpe, 2011; Rossion and Caharel, 2011).

Causal significance of upright face-preferential high-gamma augmentation in face recognition

While category-preferential high-gamma augmentation is often inferred to be a biomarker reflecting cortical processing for recognition of a given category image, we must emphasize that the causal significance of upright face-preferential high-gamma augmentation noted in this study still remains to be determined. We presented upright face stimuli with the eyes in the center-to-upper field and the mouth in the lower field, as many of the previous studies did (Kirchner and Thorpe, 2006; Pitcher et al., 2007; Crouzet et al., 2010; Rossion and Caharel, 2011). Therefore, upright face-preferential high-gamma augmentation in the lower-order visual areas could be simply attributed to a richer physical properties of eyes-eyebrows compared to a mouth. We applied a post-hoc analysis to test this possibility, but failed to explain upright face-preferential high-gamma augmentation by predominant ECoG sampling from the sites below the calcarine fissure. Further studies on a larger number of participants are necessary to determine the causal role of upright-face-preferential high-gamma augmentation within lower-order visual areas upon face detection or recognition, possibly by correlating category-preferential high-gamma augmentation and the effect of direct stimulation on face detection or recognition tasks. Unlike TMS, electrical stimulation via subdural electrodes can be delivered to a small region in the medial-inferior surfaces of the occipital lobes (Kumar et al., 2012; Parvizi et al., 2012).

Given the limited sample possible in ECoG studies, we are not able to make strong interpretations regarding the developmental effects in our measurements. Moreover, based on this study it is not possible to infer whether our ECoG findings derived from older children would be generalizable to infant or adult populations. In the present study, regardless of age, all study patients equally appeared engaged to the task. Our previous ECoG study of 77 patients failed to find a significant difference in the spectral frequency of language-related high-gamma activities across ages from 4 to 56 (Kojima et al., 2013c). Neuroimaging studies have demonstrated a protracted development of higher-order face-selective regions through late childhood and into adolescence, with a trajectory of increasing face-selectivity with increasing age that plateaus by early adulthood (Scherf et al., 2007; Golarai et al., 2010). If this developmental pattern generalizes to face-specific effects elsewhere in the brain, we might expect that adults would show the same or greater high-gamma augmentation for upright over inverted faces in lower-order visual cortex than we observed in our patients, whereas younger children and infants might be expected to show less. However, further studies of a larger number of patients across

variable age groups would be necessary to conclusively determine how the high-gamma augmentation effects described here may generalize to other stages of development.

Other methodological considerations

Our ECoG studies inevitably suffer from sampling limitations, and we were unable to exclude variability in spatial sampling across participants. The location of subdural electrode placement was purely determined by the clinical needs (Asano et al., 2009a); several subdural strip electrodes were placed in the occipital and temporal regions in order to determine the boundary between the epileptogenic zone and eloquent visual areas. Placement of larger grid electrodes in the occipital lobe was not indicated in any of our patient cohort. Nonetheless, all patients showed similar spatial patterns in high-gamma augmentation elicited by central- and peripheral-field checkerboard pattern stimuli (Fig. 3). Large high-gamma augmentation elicited by central-field stimuli was noted in the occipital pole, whereas that by peripheral-field stimuli was noted in the more anterior-medial occipital region. Electrodes located in the fusiform gyri, traditionally considered to be a part of higher-order visual areas (Kanwisher et al., 1997; Gauthier et al., 1999; Parvizi et al., 2012), did not show large high-gamma augmentation elicited by such a simple checkerboard stimuli.

Another limitation of ECoG studies is the challenge of recruiting participants. The present ECoG study, like many others using this technique, is based on data from a limited number of participants. Although these sample sizes constrain our ability to draw conclusions, it is worth noting that measurement of ECoG high-gamma augmentation represents up to a 100-fold improvement in signal-to-noise ratio over scalp EEG recording (Ball et al., 2009). Thus, many ECoG studies of less than 10 patients, using a repeated measurement approach, benefited from sufficient power to observe statistically significant effects on visually-related high-gamma measures (Lachaux et al., 2005; Miller et al., 2009).

We localized lower-order visual sites using a bipolar stimulation method (Asano et al., 2009b; Kumar et al., 2012). Because patient participation time was limited, we were unable to determine whether either or both of the electrodes within each pair were responsible for generation of phosphene; thus, we are unable to exclude the possibility that a small subset of non-eloquent sites may have been mistakenly chosen as a lower-order visual site in the present study. Nonetheless, all patients shared a similar spatial pattern in lower-order visual areas defined by electrical stimulation. Phosphenes were most frequently elicited by stimulation of electrode pairs located in either lingual or lateral occipital sites. We still don't know whether eliciting phosphenes via electrical stimulation is an equally sensitive method for localization of lower-order visual sites across occipital regions. We noted that electrical stimulation of the occipital pole often resulted in perception of a small phosphene (e.g., the size of a ladybug) in the central visual field, whereas stimulation of more anterior-medial occipital areas resulted in perception of a larger phosphene (e.g., the size of a tennis ball) in the more peripheral visual field. Very anterior-medial lingual–cuneus regions were often associated with stimulation-induced phosphenes in a far peripheral field but not with checkerboard stimuli-related high-gamma augmentation. We suspect that such regions could not be effectively activated by annular checkerboard stimuli presented in a regular LCD monitor.

Acknowledgment

This work was supported by NIH grant NS64033 (to E. Asano) as well as the intramural grant from Children's Hospital of Michigan Foundation (to E. Asano). We are grateful to Harry T. Chugani, MD, Sandeep Sood, MD, Csaba Juhász, MD, PhD, Robert Rothermel, PhD, Yutaka Nonoda, MD, Nicole Goellnitz, RN, MSN, CPNP, and Carol Pawlak, REEG/EPT at Children's Hospital of Michigan, Wayne State University for the collaboration and assistance in performing the studies described above.

Appendix A. Supplementary data

Supplementary data to this article can be found online at http://dx.doi.org/10.1016/j.neuroimage.2015.01.015.

References

Alkonyi, B., Juhász, C., Muzik, O., Asano, E., Saporta, A., Shah, A., Chugani, H.T., 2009. Quantitative brain surface mapping of an electrophysiologic/metabolic mismatch in human neocortical epilepsy. Epilepsy Res. 87, 77–87.
Amunts, K., Malikovic, A., Mohlberg, H., Schormann, T., Zilles, K., 2000. Brodmann's areas 17 and 18 brought into stereotaxic space—where and how variable? Neuroimage 11, 66–84.
Asano, E., Juhász, C., Shah, A., Sood, S., Chugani, H.T., 2009a. Role of subdural electrocorticography in prediction of long-term seizure outcome in epilepsy surgery. Brain 132, 1038–1047.
Asano, E., Nishida, M., Fukuda, M., Rothermel, R., Juhász, C., Sood, S., 2009b. Differential visually-induced gamma-oscillations in human cerebral cortex. Neuroimage 45, 477–489.
Ball, T., Kern, M., Mutschler, I., Aertsen, A., Schulze-Bonhage, A., 2009. Signal quality of simultaneously recorded invasive and non-invasive EEG. Neuroimage 46, 708–716.
Birmingham, E., Meixner, T., Iarocci, G., Kanan, C., Smilek, D., Tanaka, J.W., 2013. The moving window technique: a window into developmental changes in attention during facial emotion recognition. Child Dev. 84, 1407–1424.
Brown, E.C., Rothermel, R., Nishida, M., Juhász, C., Muzik, O., Hoechstetter, K., Sood, S., Chugani, H.T., Asano, E., 2008. In vivo animation of auditory-language-induced gamma-oscillations in children with intractable focal epilepsy. Neuroimage 41, 1120–1131.
Crouzet, S.M., Thorpe, S.J., 2011. Low-level cues and ultra-fast face detection. Front. Psychol. 2, 342.
Crouzet, S.M., Kirchner, H., Thorpe, S.J., 2010. Fast saccades toward faces: face detection in just 100 ms. J. Vis. 10, 16.1–16.17.
Dalal, S.S., Edwards, E., Kirsch, H.E., Barbaro, N.M., Knight, R.T., Nagarajan, S.S., 2008. Localization of neurosurgically implanted electrodes via photograph-MRI-radiograph coregistration. J. Neurosci. Methods 174, 106–115.
Dekaban, A.S., Sadowsky, D., 1978. Changes in brain weights during the span of human life: relation of brain weights to body heights and body weights. Ann. Neurol. 4, 345–356.
Desikan, R.S., Ségonne, F., Fischl, B., Quinn, B.T., Dickerson, B.C., Blacker, D., Buckner, R.L., Dale, A.M., Maguire, R.P., Hyman, B.T., Albert, M.S., Killiany, R.J., 2006. An automated labeling system for subdividing the human cerebral cortex on MRI scans into gyral based regions of interest. Neuroimage 31, 968–980.
Ekman, P., Friesen, W., 1976. Pictures of Facial Affect. Consulting Psychologists Press, Palo Alto, CA.
Engell, A.D., McCarthy, G., 2010. Selective attention modulates face-specific induced gamma oscillations recorded from ventral occipitotemporal cortex. J. Neurosci. 30, 8780–8786.
Farah, M.J., Wilson, K.D., Drain, M., Tanaka, J.N., 1998. What is "special" about face perception? Psychol. Rev. 105, 482–498.
Fletcher-Watson, S., Findlay, J.M., Leekam, S.R., Benson, V., 2008. Rapid detection of person information in a naturalistic scene. Perception 37, 571–583.
Fukuda, M., Nishida, M., Juhász, C., Muzik, O., Sood, S., Chugani, H.T., Asano, E., 2008. Short-latency median-nerve somatosensory-evoked potentials and induced gamma-oscillations in humans. Brain 131, 1793–1805.
Gauthier, I., Tarr, M.J., Anderson, A.W., Skudlarski, P., Gore, J.C., 1999. Activation of the middle fusiform 'face area' increases with expertise in recognizing novel objects. Nat. Neurosci. 2, 568–573.
Golarai, G., Liberman, A., Yoon, J.M.D., Grill-Spector, K., 2010. Differential development of the ventral visual cortex extends through adolescence. Front. Hum. Neurosci. http://dx.doi.org/10.3389/neuro.09.080.2009.
Haxby, J.V., Ungerleider, L.G., Clark, V.P., Schouten, J.L., Hoffman, E.A., Martin, A., 1999. The effect of face inversion on activity in human neural systems for face and object perception. Neuron 22, 189–199.
Hochberg, J., Galper, R.R., 1967. Recognition of faces: an explanatory study. Psychol. Sci. 9, 619–620.
Hoechstetter, K., Bornfleth, H., Weckesser, D., Ille, N., Berg, P., Scherg, M., 2004. BESA source coherence: a new method to study cortical oscillatory coupling. Brain Topogr. 16, 233–238.
Horton, J.C., Hoyt, W.F., 1991. Quadrantic visual field defects. A hallmark of lesions in extrastriate (V2/V3) cortex. Brain 114, 1703–1718.
Jacobs, J., Levan, P., Châtillon, C.E., Olivier, A., Dubeau, F., Gotman, J., 2009. High frequency oscillations in intracranial EEGs mark epileptogenicity rather than lesion type. Brain 132, 1022–1037.
Kanwisher, N., McDermott, J., Chun, M.M., 1997. The fusiform face area: a module in human extrastriate cortex specialized for face perception. J. Neurosci. 17, 4302–4311.
Kim, S.E., Kim, W.S., Kim, B.G., Chung, D., Jeong, J., Lee, J.S., Tae, W.S., Hong, S.B., Lee, H.W., 2013. Spatiotemporal dynamics and functional correlates of evoked neural oscillations with different spectral powers in human visual cortex. Clin. Neurophysiol. 124, 2248–2256.
Kirchner, H., Thorpe, S.J., 2006. Ultra-rapid object detection with saccadic eye movements: visual processing speed revisited. Vision Res. 46, 1762–1776.
Kojima, K., Brown, E.C., Matsuzaki, N., Asano, E., 2013a. Animal category-preferential gamma-band responses in the lower- and higher-order visual areas: intracranial recording in children. Clin. Neurophysiol. 124, 2368–2377.

Kojima, K., Brown, E.C., Matsuzaki, N., Rothermel, R., Fuerst, D., Shah, A., Mittal, S., Sood, S., Asano, E., 2013b. Gamma activity modulated by picture and auditory naming tasks: intracranial recording in patients with focal epilepsy. Clin. Neurophysiol. 124, 1737–1744.

Kojima, K., Brown, E.C., Rothermel, R., Carlson, A., Fuerst, D., Matsuzaki, N., Shah, A., Atkinson, M., Basha, M., Mittal, S., Sood, S., Asano, E., 2013c. Clinical significance and developmental changes of auditory-language-related gamma activity. Clin. Neurophysiol. 124, 857–869.

Korzeniewska, A., Franaszczuk, P.J., Crainiceanu, C.M., Kuś, R., Crone, N.E., 2011. Dynamics of large-scale cortical interactions at high gamma frequencies during word production: event related causality (ERC) analysis of human electrocorticography (ECoG). Neuroimage 56, 2218–2237.

Kumar, G., Juhász, C., Sood, S., Asano, E., 2012. Olfactory hallucinations elicited by electrical stimulation via subdural electrodes: effects of direct stimulation of olfactory bulb and tract. Epilepsy Behav. 24, 264–268.

Lachaux, J.P., George, N., Tallon-Baudry, C., Martinerie, J., Hugueville, L., Minotti, L., Kahane, P., Renault, B., 2005. The many faces of the gamma band response to complex visual stimuli. Neuroimage 25, 491–501.

Levy, I., Hasson, U., Avidan, G., Hendler, T., Malach, R., 2001. Center-periphery organization of human object areas. Nat. Neurosci. 4, 533–539.

Matsuzaki, N., Nagasawa, T., Juhász, C., Sood, S., Asano, E., 2012. Independent predictors of neuronal adaptation in human primary visual cortex measured with high-gamma activity. Neuroimage 59, 1639–1646.

Mendola, J.D., Buckthought, A., 2013. fMRI investigation of monocular pattern rivalry. J. Cogn. Neurosci. 25, 62–73.

Miller, K.J., Makeig, S., Hebb, A.O., Rao, R.P., denNijs, M., Ojemann, J.G., 2007. Cortical electrode localization from X-rays and simple mapping for electrocorticographic research: the "location on cortex" (LOC) package for MATLAB. J. Neurosci. Methods 162, 303–308.

Miller, K.J., Hermes, D., Schalk, G., Ramsey, N.F., Jagadeesh, B., den Nijs, M., Ojemann, J.G., Rao, R.P., 2009. Detection of spontaneous class-specific visual stimuli with high temporal accuracy in human electrocorticography. Conf. Proc. IEEE Eng. Med. Biol. Soc. 2009, 6465–6468.

Murphey, D.K., Maunsell, J.H., Beauchamp, M.S., Yoshor, D., 2009. Perceiving electrical stimulation of identified human visual areas. Proc. Natl. Acad. Sci. U. S. A. 106, 5389–5393.

Muzik, O., Chugani, D.C., Zou, G., Hua, J., Lu, Y., Lu, S., Asano, E., Chugani, H.T., 2007. Multimodality data integration in epilepsy. Int. J. Biomed. Imaging http://dx.doi.org/10.1155/2007/13963.

Nagasawa, T., Matsuzaki, N., Juhász, C., Hanazawa, A., Shah, A., Mittal, S., Sood, S., Asano, E., 2011. Occipital gamma-oscillations modulated during eye movement tasks: simultaneous eye tracking and electrocorticography recording in epileptic patients. Neuroimage 58, 1101–1109.

Papp, N., Ktonas, P., 1977. Critical evaluation of complex demodulation techniques for the quantification of bioelectrical activity. Biomed. Sci. Instrum. 13, 135–145.

Parvizi, J., Jacques, C., Foster, B.L., Witthoft, N., Rangarajan, V., Weiner, K.S., Grill-Spector, K., 2012. Electrical stimulation of human fusiform face-selective regions distorts face perception. J. Neurosci. 32, 14915–14920.

Pieters, T.A., Conner, C.R., Tandon, N., 2013. Recursive grid partitioning on a cortical surface model: an optimized technique for the localization of implanted subdural electrodes. J. Neurosurg. 118, 1086–1097.

Pitcher, D., Walsh, V., Yovel, G., Duchaine, B., 2007. TMS evidence for the involvement of the right occipital face area in early face processing. Curr. Biol. 17, 1568–1573.

Puce, A., Allison, T., Gore, J.C., McCarthy, G., 1995. Face-sensitive regions in human extrastriate cortex studied by functional MRI. J. Neurophysiol. 74, 1192–1199.

Quinn, P.C., Eimas, P.D., 1998. Evidence for a global categorical representation of humans by young infants. J. Exp. Child Psychol. 69, 151–174.

Quinn, P.C., Doran, M.M., Reiss, J.E., Hoffman, J.E., 2009. Time course of visual attention in infant categorization of cats versus dogs: evidence for a head bias as revealed through eye tracking. Child. Dev. 80, 151–161.

Ray, S., Crone, N.E., Niebur, E., Franaszczuk, P.J., Hsiao, S.S., 2008. Neural correlates of high-gamma oscillations (60–200 Hz) in macaque local field potentials and their potential implications in electrocorticography. J. Neurosci. 28, 11526–11536.

Rossion, B., Caharel, S., 2011. ERP evidence for the speed of face categorization in the human brain: disentangling the contribution of low-level visual cues from face perception. Vision Res. 51, 1297–1311.

Salmelin, R., Hari, R., 1994. Spatiotemporal characteristics of sensorimotor neuromagnetic rhythms related to thumb movement. Neuroscience 60, 537–550.

Scherf, K.S., Behrmann, M., Humphreys, K., Luna, B., 2007. Visual category-selectivity for faces, places, and objects emerges along different developmental trajectories. Dev. Sci. 10, F15–F30.

Schneider, W., Noll, D.C., Cohen, J.D., 1993. Functional topographic mapping of the cortical ribbon in human vision with conventional MRI scanners. Nature 365, 150–153.

Summerfield, C., Egner, T., Mangels, J., Hirsch, J., 2006. Mistaking a house for a face: neural correlates of misperception in healthy humans. Cereb. Cortex 16, 500–508.

Uematsu, M., Matsuzaki, N., Brown, E.C., Kojima, K., Asano, E., 2013. Human occipital cortices differentially exert saccadic suppression: intracranial recording in children. Neuroimage 83, 224–236.

Vaidya, A.R., Jin, C., Fellows, L.K., 2014. Eye spy: the predictive value of fixation patterns in detecting subtle and extreme emotions from faces. Cognition 133, 443–456.

Valenza, E., Simion, F., Cassia, V.M., Umiltà, C., 1996. Face preference at birth. J. Exp. Psychol. Hum. Percept. Perform. 22, 892–903.

Vidal, J.R., Ossandón, T., Jerbi, K., Dalal, S.S., Minotti, L., Ryvlin, P., Kahane, P., Lachaux, J.P., 2010. Category-specific visual responses: an intracranial study comparing gamma, beta, alpha, and ERP response selectivity. Front. Hum. Neurosci. 2010. http://dx.doi.org/10.3389/fnhum.2010.00195.

Wellmer, J., von Oertzen, J., Schaller, C., Urbach, H., König, R., Widman, G., Van Roost, D., Elger, C.E., 2002. Digital photography and 3D MRI-based multimodal imaging for individualized planning of resective neocortical epilepsy surgery. Epilepsia 43, 1543–1550.

Woods, D.L., Yund, E.W., Kang, X.J., 2003. Unified functional/anatomical maps of human auditory cortex. Archives of Neurobehavioral Experiments and Stimuli 46 (Link to: http://www.neurobs.com/ex_files/expt_view?id=46).

Wu, H.C., Nagasawa, T., Brown, E.C., Juhasz, C., Rothermel, R., Hoechstetter, K., Shah, A., Mittal, S., Fuerst, D., Sood, S., Asano, E., 2011. γ-Oscillations modulated by picture naming and word reading: intracranial recording in epileptic patients. Clin. Neurophysiol. 122, 1929–1942.

Yin, R.K., 1969. Looking at upside-down faces. J. Exp. Psychol. 81, 141–145.

Yoshor, D., Bosking, W.H., Ghose, G.M., Maunsell, J.H., 2007. Receptive fields in human visual cortex mapped with surface electrodes. Cereb. Cortex 17, 2293–2302.

Yovel, G., Kanwisher, N., 2004. Face perception: domain specific, not process specific. Neuron 44, 889–898.

Zijlmans, M., van Eijsden, P., Ferrier, C.H., Kho, K.H., van Rijen, P.C., Leijten, F.S., 2009. Illusory shadow person causing paradoxical gaze deviations during temporal lobe seizures. J. Neurol. Neurosurg. Psychiatry 80, 686–688.